Journal of the European Ceramic Society **17** (1997) 203–209

PII: S0955-2219(96)00108-2
0955-2219/97/$17.00

Thermal Debinding of Injection Moulded Ceramics

M. Trunec & J. Cihlář

Department of Ceramics, Technical University of Brno, Technická 2, 616 69 Brno, Czech Republic

(Received 15 September 1995; accepted 10 June 1996)

Abstract

Special equipment for thermal removal of binder under controlled pressure conditions and with controlled gas flow rate was built to study the debinding process of injection moulded parts. The equipment was designed to record changes in the weight of injection mouldings, and an operating system made it possible to control their weight loss by temperature. The thermal debinding process of injection moulded parts prepared from fine alumina powder and a thermoplastic binder system based on ethylene–vinyl acetate copolymer and paraffin was studied using this equipment. The influence of pressure and flow rate of various gaseous atmospheres (air, oxygen, nitrogen, carbon dioxide and vacuum) was investigated. The benefit of binder removal in an inert atmosphere with controlled weight loss rate is described. © 1996 Elsevier Science Limited.

1 Introduction

Injection moulding of ceramic powders is an attractive method for the production of complex-shaped parts with a high degree of precision.[1,2] A key moment in this technology is the removal of organic binder from the injection moulded parts prior to their sintering. This operation often gives rise to defects, especially in the case when fine ceramic powder is used[3] or parts with large cross-sections are produced.[4] Thermal treatment appears to be the most viable method of binder removal for mass production of parts, because of the simplicity of the method and equipment.[5] The mechanism of extraction includes evaporation of low-molecular-weight components without degrading the polymeric chain.[6] In inert atmosphere the thermal degradation of polymers with higher molecular weight takes place at all points throughout the body. The thermal degradation of polyolefins as well as of other vinyl-type polymers was found to occur predominantly by random scission and this process was explained on the basis of a free-radical mechanism.[7] Elimination of side radicals for vinyl-type polymers is another mechanism of thermal degradation.[8] The volatile products of degradation and depolymerization diffuse towards the surface and evaporate.[6] However, mass transport by diffusion in molten binder is limited.[9] If the diffusion flux of degradation products from the centre of the body towards the surface and their evaporation are not fast enough, the concentration of degradation products in the binder may reach a limit state. This results in the generation of gases inside the body and thus in the appearance of defects.[10,11] If oxygen is present, oxidative degradation takes place at the liquid binder/gas atmosphere interface. Oxidation is limited to the surface layer, the thickness of which is given by oxygen diffusion in the molten binder and in its degradation products.[12,13] This process is described by the shrinking unreacted core model.[14] The oxidative degradation followed by volatilization of degradation products recedes to the body centre and reduces the effective dimensions of the component. Thus diffusion distances from the body centre to the unsaturated surface are reduced. Simultaneously with oxidative degradation thermal degradation takes place throughout the volume of the body. The weight loss–temperature profile is therefore dependent on the sample dimensions.[12] The internal thermal degradation is a high activation energy process (150–200 kJ mol^{-1}). The oxidative degradation, on the other hand, is a lower activation energy process (30–40 kJ mol^{-1}) including autocatalytic oxidation initiated by hydroperoxide groups and tends to dominate at lower temperatures.[6] If the successive binder removal from the surface to the body centre by oxidative degradation creates a brittle surface layer while the core is still plastic, non-uniform shrinkage can result in defects.[15]

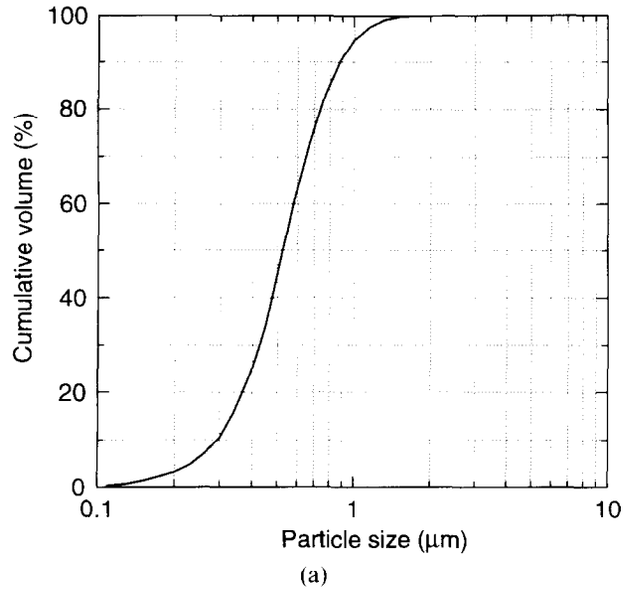

(a)

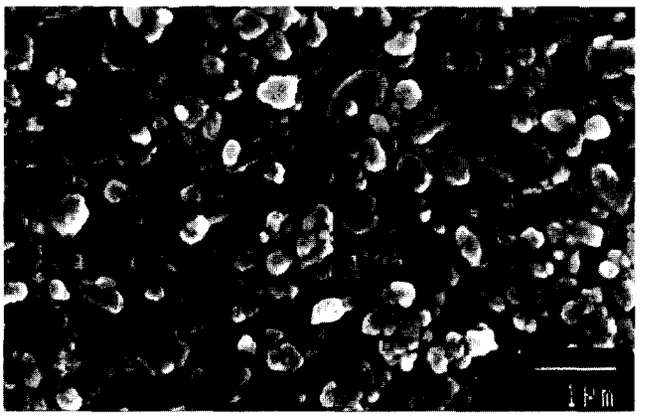

(b)

Fig. 1. (a) Particle size distribution and (b) SEM micrograph of alumina powder.

Because of the great number of parameters affecting the binder removal process, e.g. binder composition, characteristics of ceramic powder, nature and pressure of gas atmosphere, rate of heating, shape of component part, etc., it is difficult to determine a general debinding cycle of thermal extraction — debinding conditions have to be determined individually for every single case. The present work is concerned with the effect of gas atmosphere on the binder removal from a ceramic green body from the point of view of obtaining defect-free parts. In order to clarify and evaluate the process taking place in the specimens under extraction, the changes in the weight of injection moulded parts were followed and examined.

2 Experimental

2.1 Preparation of injection mouldings

Used for the preparation of ceramic suspension was alumina powder, type RC-HP DBM, supplied by Reynolds Chemicals; its mean particle size was 0·53 μm. The particle size distribution curve and a microphotograph of the powder used are shown in Figs 1(a) and 1(b).

Table 1. Composition of ceramic suspension

	wt%
Alumina	86·45
Elvax 250	4·60
Elvax 260	2·30
Paraffin	4·60
Stearic acid	1·20
Oleic acid	0·85

The binder comprised ethylene–vinyl acetate copolymer (EVA), types Elvax 250 and 260 (Du Pont de Nemours), and type 52/54 paraffin (Koramo). Stearic and oleic acids were used as processing aids.

The composition of the ceramic suspension is given in Table 1. The volume loading of ceramic powder in the suspension was 59·8 vol%. Prior to mixing with the binder, the ceramic material with stearic and oleic acids was dry-milled in a ball mill for a period of 24 h. The ceramic suspension was mixed in a double-blade mixer (HKD 0·6T, IKA WERK) at a temperature of 130°C for 90 min.

Specimens were prepared by injection moulding on a reciprocating screw injection moulding machine (Allrounder 220 M, Arburg); they were of cylindrical shape, diameter 5·8 mm and length 25 mm. Injection moulding conditions are given in Table 2.

2.2 Binder removal

Special equipment was designed for the thermal debinding of ceramic green bodies which made it possible to remove the binder under controlled pressure conditions (5 Pa–10^5 Pa) and with controlled flow rate of the gas atmosphere chosen. A schematic drawing of the debinding furnace is shown in Fig. 2. With this equipment changes in the weight of extracted injection moulded parts could be determined with a resolution of 1 mg. A computer control system provided for temperature control to a required weight loss. The mass of the injection moulded parts under test ranged from 5 to 15 g (the maximum possible mass was 200 g). To control temperature according to the rate of

Table 2. Injection moulding conditions

Injection flow (cm^3 s^{-1})	15
Holding pressure (MPa)	60
Barrel temperatures (°C) (feed to nozzle)	140–150–155 160–160
Mould temperature (°C)	30
Cooling time (s)	25

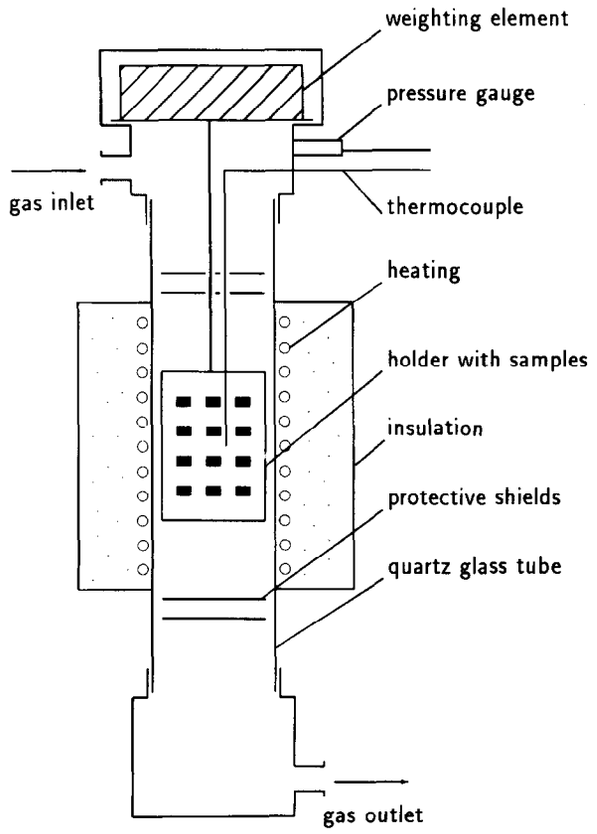

Fig. 2. Schematic drawing of the debinding furnace.

weight loss of extracted bodies, a modified version was used of the algorithm proposed by Johnsson *et al.*[16] The improvement of this algorithm and the design of debinding furnace made it possible to obtain a better control of the rate of weight loss, with almost monotonous increase in temperature instead of the staggered nature of temperature as given by Johnsson *et al.*

The weight loss was followed under a linear heating of 10°C h^{-1} in air, oxygen, nitrogen (O_2 < 50 ppm) and carbon dioxide, always at a gas flow rate of 200 cm^3 min^{-1}, and in vacuum (5·5–6 Pa). In nitrogen atmosphere binder removal was also carried out at a flow rate of 800 cm^3 min^{-1}, and without flow. For the binder removal in air, static atmosphere was also used. Temperature was increased as long as there was any loss of weight. In nitrogen atmosphere the extraction was performed with the temperature controlled to give a constant rate of weight loss of ceramic specimens. The maximum admissible value of the rate of heating was set at 35°C h^{-1}, and the maximum value of the rate of loss of weight was such as to obtain specimens free from defects. For comparison a debinding cycle was carried out with linear temperature increase; its duration corresponded to the cycle with controlled loss of weight.

Apart from the above equipment for debinding, a hot-air drier was used with program-controlled air temperature. The air in the drier was renewed

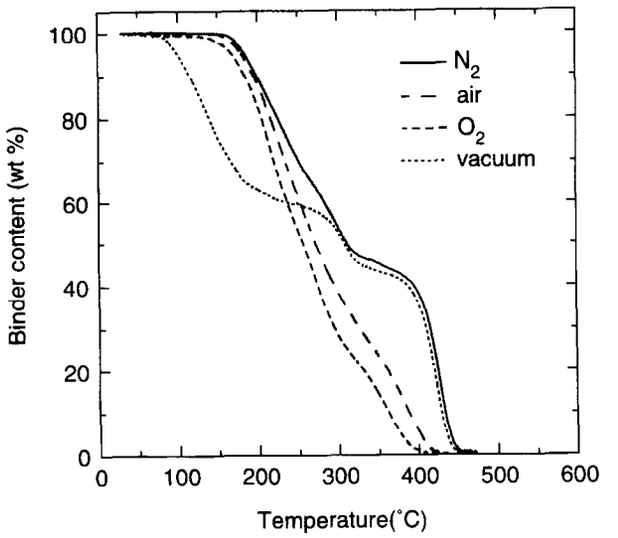

Fig. 3. Weight loss curves for specimens during binder removal at a heating rate of 10°C h^{-1} in nitrogen, oxygen and air with a gas flow of 200 cm^3 min^{-1}, and in vacuum.

continuously at a rate of several dm^3 h^{-1}. Ceramic specimens were extracted at a linear heating of 3 and 10°C h^{-1}. The specimens were taken out successively at intervals of 30°C so that the area of the beginning of defect formation could be determined. In the case of heating at 10°C h^{-1} isothermal holds of 24 h at 150, 160 and 175°C were also included, after which the bodies were cooled and examined.

Extracted specimens were examined visually, by means of scanning electron microscopy (SEM) and by X-ray radiography. Some specimens were presintered at 1000°C to avoid damage during handling. X-ray radiography was also used to establish the absence of defects in injection moulded ceramic parts prior to binder removal.

3 Results and Discussion

A comparison of weight losses during the debinding of ceramic specimens at a heating rate of 10°C h^{-1} in different atmospheres with a gas flow of 200 cm^3

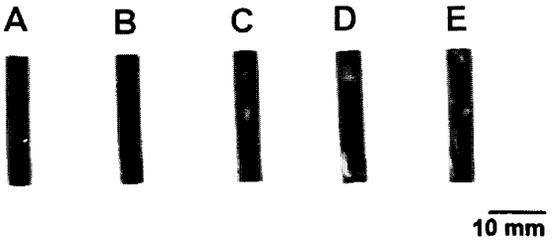

Fig. 4. Print of X-ray radiograph of ceramic specimens after binder removal at a heating rate of 10°C h^{-1} in various atmospheres with a gas flow of 200 cm^3 min^{-1}, and in vacuum: (A) nitrogen, (B) carbon dioxide, (C) vacuum, (D) air and (E) oxygen.

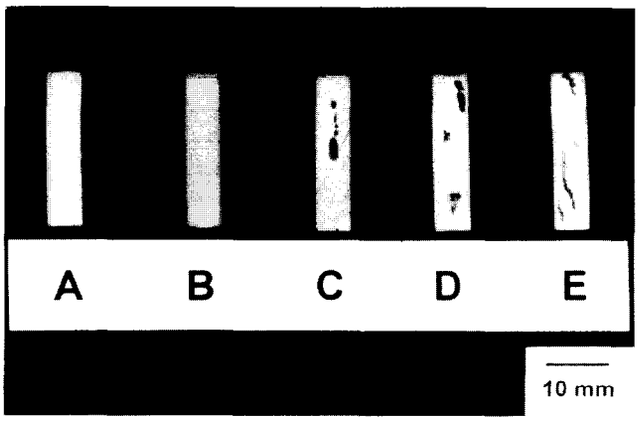

Fig. 5. Appearance of defects on polished longitudinal sections of presintered specimens after binder removal at a heating rate of 10°C h^{-1} in various atmospheres with a gas flow of 200 cm^3 min^{-1}, and in vacuum: (A) nitrogen, (B) carbon dioxide, (C) vacuum, (D) air and (E) oxygen.

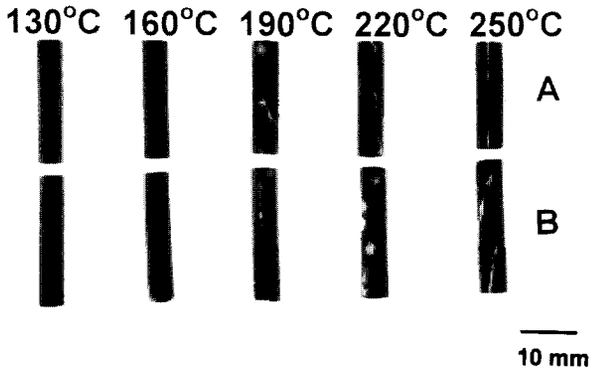

Fig. 7. Print of X-ray radiograph of ceramic specimens after binder removal heated to 130, 160, 190, 220 and 250°C at a heating rate of (A) 3°C h^{-1} and (B) 10°C h^{-1} in air atmosphere.

min^{-1} and under vacuum is shown in Fig. 3. The nature of resulting defects can be seen from the X-ray radiograph of extracted specimens (Fig. 4) and from Fig. 5, which shows the longitudinal sections of presintered specimens.

Binder removal in air atmosphere at a heating rate of 10°C h^{-1} was accompanied by almost linear weight loss in the temperature range from 150 to 420°C. A small difference in the recorded weight loss was established between static air atmosphere and that with an air flow of 200 cm^3 min^{-1} (Fig. 6). The air flow slightly increased the weight loss. The air flow corresponded to an atmosphere flow rate of 25.5 mm min^{-1}. In both cases the specimens displayed defects. Two types of defect were found — slight bloating with large voids in the specimen centre and cracks below the specimen surface. It has been found that defect-free extracted specimens cannot be obtained either at heating rate of 3°C h^{-1} or at heating rate of 10°C h^{-1} with isothermal holds at temperatures of 150, 160 and 175°C. Defects appeared even during isothermal holds. Figure 7 is a print of X-ray radiographs of specimens that were extracted to different temperatures with a heating rate of 3 and 10°C h^{-1}. It is clear that in both cases defects appeared already in the temperature range 160–190°C. The loss in weight recorded when removing the binder in pure oxygen with a flow rate of 200 cm^3 min^{-1} and a temperature increase of 10°C h^{-1} was speeded up compared with the situation concerning the loss in weight in air atmosphere. The nature of defects in extracted bodies was similar but the defects were more pronounced.

The loss in weight under vacuum (5·5–6 Pa) differed from the previous cases. With a heating rate of 10°C h^{-1} the temperature range of binder removal increased to the interval from 80 to 450°C,

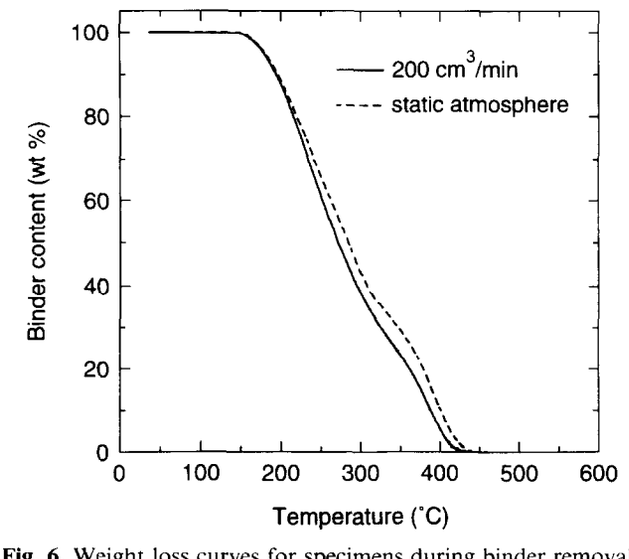

Fig. 6. Weight loss curves for specimens during binder removal at a heating rate of 10°C h^{-1} in static air atmosphere and in air flow of 200 cm^3 min^{-1}.

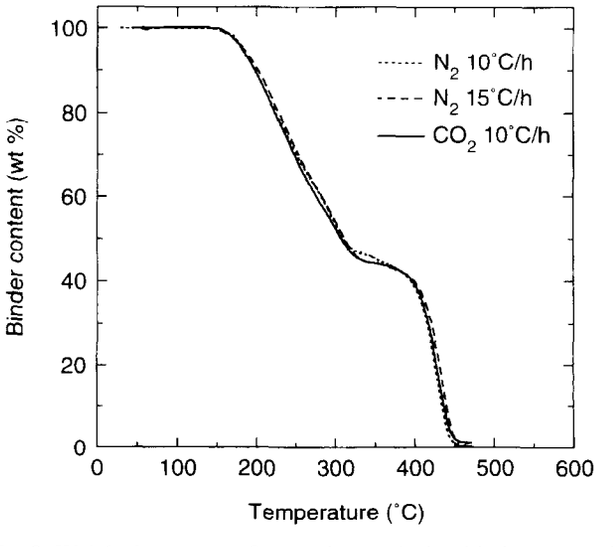

Fig. 8. Weight loss curves for specimens during binder removal at a heating rate of 10 and 15°C h^{-1} in nitrogen and 10°C h^{-1} in carbon dioxide atmospheres, both with a gas flow of 200 cm^3 min^{-1}.

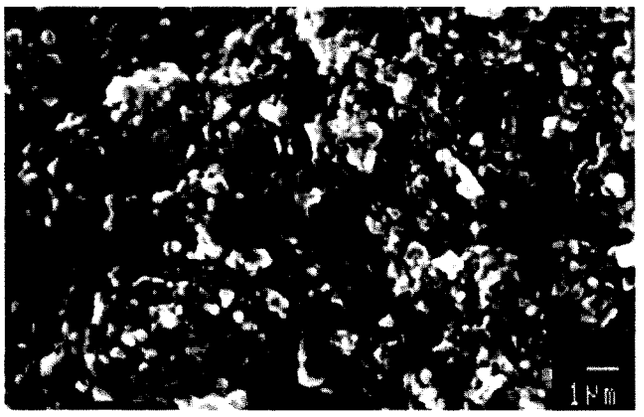

Fig. 9. SEM photomicrograph of fracture surface of oxidized surface layer of a specimen after binder removal to 220°C at a heating rate of 10°C h^{-1} in oxygen.

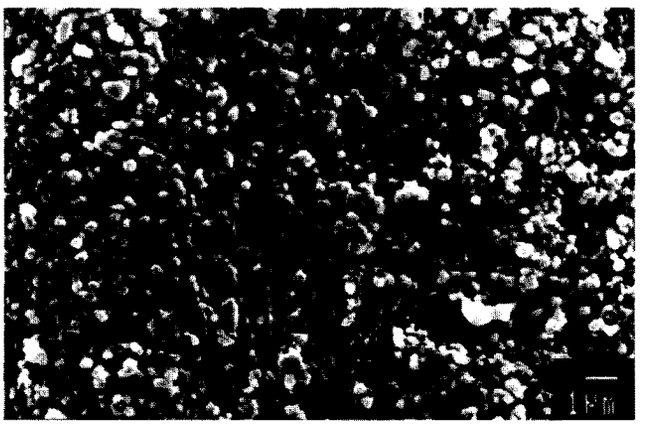

Fig. 11. SEM photomicrograph of fracture surface of a presintered specimen debinded at a heating rate of 10°C h^{-1} in oxygen.

and the binder was removed in several marked steps. In this type of extracted specimen voids and cracks were found in the specimen centre.

Defect-free extracted specimens were obtained by removing the binder in nitrogen atmosphere with the temperature increasing by 10°C h^{-1}. The binder was removed in two marked temperature regions. The first was in the range from 150 to 320°C, the other in the range from 400 to 450°C. There was no pronounced difference between the recorded values of weight loss of extracted specimens for different nitrogen flow rates (0, 200 and 800 cm^3 min^{-1}). With the heating rate increased to 15°C h^{-1} and a flow rate of 200 cm^3 min^{-1} the temperature stages of a binder removal were the same (Fig. 8). In specimens exposed to this faster debinding cycle cracks were found in the specimen centre.

Binder removal in CO_2 atmosphere had a similar course to that in nitrogen atmosphere (Fig. 8). Defect-free specimens were also obtained. However, the bodies after binder removal were bright, similar to the specimens extracted in air and oxygen. By contrast, specimens extracted in vacuum were grey and those extracted in nitrogen were grey-black.

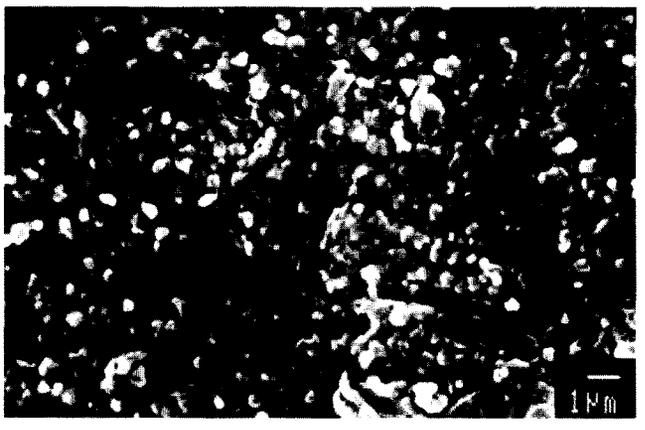

Fig. 10. SEM photomicrograph of fracture surface of unreacted core of a specimen after binder removal to 220°C at a heating rate of 10°C h^{-1} in oxygen.

At higher temperatures (> 400°C) in CO_2 atmosphere carbon dioxide probably caused oxidation of the carbon residue of binder, which gave rise to gaseous products. However, due to the small amount of carbon residues at reaction temperature, this oxidation did not affect the record of weight loss.

A comparison of weight losses during the debinding of ceramic specimens in different atmospheres has shown that oxygen in the atmosphere speeded up binder removal caused by oxidative degradation. Increased binder removal by oxidative degradation was observed especially in the case of higher mass losses when, due to the developing porosity[17] and especially to the developing cracks and voids, there was an increase in the area of the liquid binder/oxidizing atmosphere interface. At the liquid binder/oxidizing atmosphere interface a layer of non-volatile products of oxidative degradation appeared. The thickness of this layer increased with temperature and with debinding time at isothermal holds in oxygen-containing atmosphere. Figures 9, 10 and 11 give the microstructures of the oxidized layer and the unreacted core at 220°C in oxygen atmosphere, and the microstructure of the presintered specimen. The microphotographs show that oxidation products remained in the surface layer and there was no structure with interconnected porosity, which can be seen in the presintered specimen. These oxidation products burnt out later in the process at higher temperature (350–400°C). The layer of products of oxidative degradation probably slowed down the diffusion of components with low molecular weight and volatile products of thermal degradation from inside the specimen towards the surface and their evaporation, leading to their limit concentration in the specimen centre being exceeded, to the appearance of the gas phase and the appearance of defects due to the pressure of gas components. The shrinkage differences

Fig. 12. Photomicrograph of a subsurface crack on fracture surface of a specimen after binder removal to 220°C at a heating rate of 10°C h^{-1} in oxygen.

between the superficial oxidized layer and the unreacted core led to the appearance of subsurface cracks. The cracks in the cross-section of specimens extracted in oxidizing atmosphere determine the thickness of the oxidized layer at the moment when, due to binder removal and its degradation, the specimens lost their plastic nature (Fig. 12). The layer thickness along the circumference was not constant. The possible mechanism of formation of oxidation products of the binder on the ethylene–vinyl acetate copolymer base included:

1. Forming of radicals

$$\sim\!\!\sim CH(OCOCH_3)\text{–}CH_2\text{–}CH_2\,CH_2\,CH_2\sim\!\!\sim + O_2 \longrightarrow$$

$$\sim\!\!\sim CH(OCOCH_3)\text{–}CH_2\text{–}CH_2\text{–}\dot{C}H\text{–}CH_2\sim\!\!\sim + HOO^{\cdot}$$

2. Chain breaking

$$\sim\!\!\sim CH(OCOCH_3)\text{–}CH_2\text{–}CH_2\text{–}\dot{C}H\text{–}CH_2\sim\!\!\sim \longrightarrow$$

$$\sim\!\!\sim CH(OCOCH_3)\text{–}CH_2^{\cdot} + CH_2{=}CH\text{–}CH_2\sim\!\!\sim$$

3. Crosslinking (molecular weight increase)

$$\sim\!\!\sim CH(OCOCH_3)\text{–}CH_2^{\cdot} + \sim\!\!\sim CH(OCOCH_3)\text{–}CH_2\text{–}CH_2\text{–}\dot{C}H\text{–}CH_2\sim\!\!\sim \longrightarrow$$

$$\sim\!\!\sim CH(OCOCH_3)\text{–}CH_2\text{–}CH_2\text{–}CH(OCOCH_3)\text{–}CH_2\sim\!\!\sim$$

$$\sim\!\!\sim CH(OCOCH_3)\text{–}CH_2\text{–}CH_2\,CH_2\text{–}CH\sim\!\!\sim$$

4. Oxidation of C–H bond (e.g. aldehyde groups forming)

$$\sim\!\!\sim CH(OCOCH_3)\text{–}CH_2^{\cdot} + {}^{\cdot}OOH \longrightarrow \sim\!\!\sim CH(OCOCH_3)\text{–}CH_2\text{–}O\text{–}OH \longrightarrow$$

$$\sim\!\!\sim CH(OCOCH_3)\text{–}CH{=}O + H_2O$$

5. Breaking of C–$OCOCH_3$ bond

$$\sim\!\!\sim CH(OCOCH_3)\text{–}CH_2\text{–}CH_2\sim\!\!\sim \longrightarrow$$

$$\sim\!\!\sim \dot{C}H\text{–}CH_2\text{–}CH_2\sim\!\!\sim + CH_3\text{–}COO^{\cdot}$$

When the binder was removed in vacuum, almost a third of the binder was removed in the temperature interval 80–150°C. The slow diffusion of volatile components in viscous polymer binder at low temperatures, and the great pressure gradient between the inside and the surface of specimen, probably caused defects in the specimens extracted in vacuum.

Increasing the heating rate in nitrogen to 15°C h^{-1} resulted in the appearance of cracks in the specimen centre. In this case the limiting factor was probably the slow diffusion flux of low-molecular-weight components and degradation products through tiny pores to the surface, where they could evaporate.

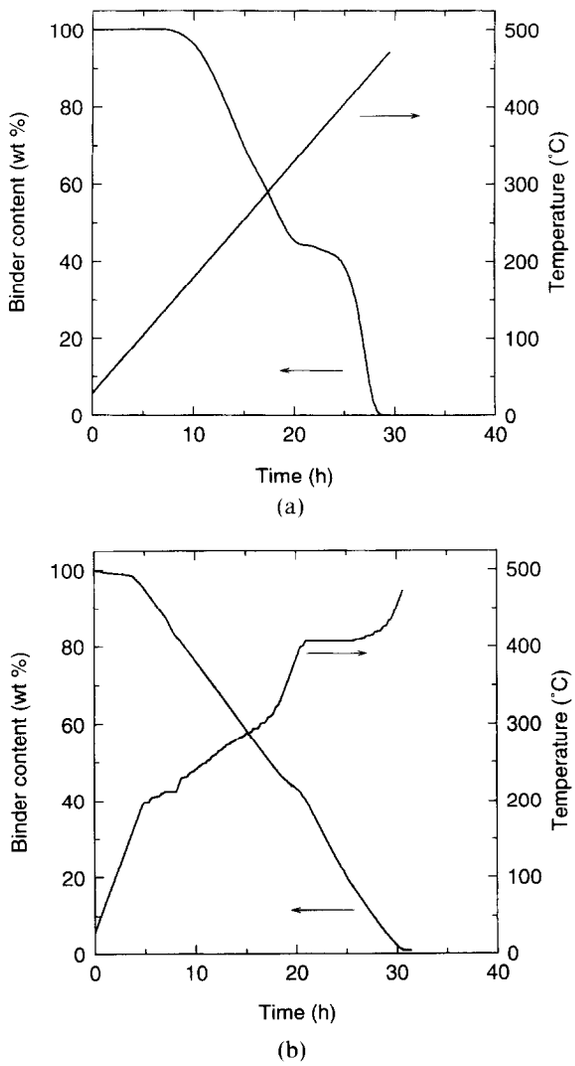

Fig. 13. Weight loss temperature–time curves for specimens during binder removal (a) with a linear heating rate of 15°C h^{-1} and (b) with a constant weight loss rate, both in nitrogen atmosphere.

The appearance of degradation products during extraction is not continuous and the diffusion conditions are not constant either, which is confirmed by non-linear weight losses of specimens extracted in nitrogen. Binder removal can thus be speeded up by controlling the temperature to yield a constant or, in the optimum case, a controlled variable weight loss rate of extracted specimens. This can cut down the danger of defects appearing due to internal pressure of degradation products and result in faster debinding cycles.

Figures 13(a) and (b) provide a comparison of the debinding cycle with a linear temperature increase of 15°C h^{-1} and the cycle with constant weight loss rate. The two cycles were of roughly the same duration. The plot of weight loss under linear heating revealed steep areas, which indicated the probability of defects being developed. Distributing the binder removal evenly over a wider area reduced the loss intensity and yielded defect-free specimens.

4 Conclusions

Thermal debinding of injection moulded specimens in an atmosphere containing oxygen did not make it possible to obtain defect-free parts. On the surface of the specimen a layer of non-volatile products was formed by oxidative degradation, thus slowing down the diffusion flux of the low-molecular-weight components and the products of thermal degradation from the specimen centre to the surface, and also slowing down their evaporation. This resulted in the generation of gases due to the boiling of low-molecular-weight components and degradation products inside the specimen, and thus in the appearance of defects. Also, the low pressure had no favourable effect on the course of binder removal and led to defects in the specimens. Binder removal in nitrogen and carbon dioxide yielded specimens free from defects. No pronounced effect of nitrogen atmosphere flows on weight loss could be observed. Controlling the temperature on the basis of weight loss in nitrogen atmosphere accelerated the process and led to the possibility of suggesting an optimum debinding cycle.

References

1. Edirisinghe, M. J. & Evans, J. R. G., Review: fabrication of engineering ceramics by injection moulding. I. Materials selection. *Int. J. High Technol. Ceram.*, **2** (1986) 1–31.
2. Edirisinghe, M. J. & Evans, J. R. G., Review: fabrication of engineering ceramics by injection moulding. II. Techniques. *Int. J. High Technol. Ceram.*, **2** (1986) 249–278.
3. Evans, J. R. G & Edirisinghe, M. J., Interfacial factors affecting the incidence of defects in ceramic mouldings. *J. Mater. Sci.*, **26** (1991) 2081–2088.
4. Zhang, J. G., Edirisinghe, M. J. & Evans, J. R. G., A catalogue of ceramic injection moulding defects and their causes. *Indust. Ceram.*, **9** (1989) 72–82.
5. German, R. M., *Powder Injection Molding*. Metal Powder Industries Federation, NJ, 1990, pp. 282–283.
6. Wright, J. K., Evans, J. R. G. & Edirisinghe, M. J., Degradation of polyolefin blends used for ceramic injection moulding. *J. Am. Ceram. Soc.*, **72** (1989) 1822–1828.
7. Seeger, M. & Gritter, R. J., Thermal decomposition and volatilization of poly(α-olefins). *J. Polym. Sci., Polym. Chem. Edn*, **15** (1977) 1393–1402.
8. Chartier, T., Ferrato, M. & Baumard, J. E., Debinding of ceramics: a review. *Ceram. Acta*, **6** (1994) 17–27.
9. Matar, S. A., Edirisinghe, M. J., Evans, J. R. G. & Twiyell, E. H., The effect of porosity development on the removal of organic vehicle from ceramic or metal mouldings. *J. Mater. Res.*, **8** (1993) 617–625.
10. Barone, M. R. & Ulicny, J. C., Liquid-phase transport during removal of organic binder in injection-molded ceramics. *J. Am. Ceram. Soc.*, **73** (1990) 3323–3333.
11. Shukla, V. N. & Hill, D. C., Binder evolution from powder compacts: thermal profile for injection-molded articles. *J. Am. Ceram. Soc.*, **72** (1989) 1797–1803.
12. Woodthorpe, J., Edirisinghe, M. J. & Evans, J. R. G., Properties of ceramic injection moulding formulation, III. Polymer removal. *J. Mater. Sci.*, **24** (1989) 1038–1048.
13 Wright, J. K. & Evans, J. R. G., Kinetics of the oxidative degradation of ceramic injection-moulding vehicle. *J Mater. Sci.*, **26** (1991) 4897 4904.
14. Szekely, J., Evans, J. W. & Sohn, H. Y., *Gas–Solid Reactions*. Academic Press, New York, 1976, pp. 65–107.
15. Quackenbush, C. L., French, K. & Neil, J. T., Fabrication of sinterable silicon nitride by injection molding. *Ceram. Eng. Sci. Proc.*, **3** (1982) 20–34.
16. Johnsson, A., Carlström, E., Hermansson, L. & Carlsson, R., Minimization of the extraction time for injection moulded ceramics. *Proc. Br. Ceram. Soc.*, **33** (1983) 139–147.
17. Shaw, H. M. & Edirisinghe, M. J., Porosity development during removal of organic vehicle from ceramic injection mouldings. *J. Eur. Ceram. Soc.*, **13** (1994) 135–142.